

Phase transition of clock models on hyperbolic lattice studied by corner transfer matrix renormalization group method

A. Gendiar¹, R. Krcmar¹, K. Ueda² and T. Nishino²

¹*Institute of Electrical Engineering, Centre of Excellence CENG,*

Slovak Academy of Sciences, Dúbravská cesta 9, SK-841 04, Bratislava, Slovakia

²*Department of Physics, Graduate School of Science, Kobe University, Kobe 657-8501, Japan*

(Dated: April 25, 2019)

Two-dimensional ferromagnetic N -state clock models are studied on a hyperbolic lattice represented by tessellation of pentagons. The lattice lies on the hyperbolic plane with a constant negative scalar curvature. We observe the spontaneous magnetization, the internal energy, and the specific heat at the center of sufficiently large systems, where the fixed boundary conditions are imposed, for the cases $N \geq 3$ up to $N = 30$. The model with $N = 3$, which is equivalent to the 3-state Potts model on the hyperbolic lattice, exhibits the first order phase transition. A mean-field like phase transition of the second order is observed for the cases $N \geq 4$. When $N \geq 5$ we observe the Schottky type specific heat below the transition temperature, where its peak height at low temperatures scales as N^{-2} . From these facts we conclude that the phase transition of classical XY-model deep inside the hyperbolic lattices is not of the Berezinskii-Kosterlitz-Thouless type.

PACS numbers: 05.50.+q, 05.70.Jk, 64.60.F-, 75.10.Hk

I. INTRODUCTION

Two-dimensional (2D) lattice models with continuous local spin symmetry, such as the classical XY-model and the classical Heisenberg model on the square lattice, do not have finite magnetization when temperature is finite. This fact proved by Mermin and Wagner [1] does not exclude the presence of phase transition of the Berezinskii-Kosterlitz-Thouless (BKT) type [2, 3]. These well-known facts are based on analysis in the flat 2D plane.

Quite recently, Baek *et al.* studied the XY model on the heptagonal lattice [4], which is one of the hyperbolic lattices constructed as a tessellation of heptagons on the hyperbolic plane, i.e., the 2D space with a constant negative curvature [5]. By way of the Monte Carlo (MC) simulations for open boundary systems, they concluded the absence of phase transition, including that of the BKT type. Their result is in accordance with the thermodynamic property of the Ising model on the hyperbolic lattice, where there is no singularity in the specific heat as shown by d'Auriac *et al.* [6]. These observations on the hyperbolic lattice can be explained by the non-negligible effect of the system boundary [7, 8], which always has a finite portion of the system regardless of the system size.

It should be noted, as pointed by d'Auriac *et al.*, that the presence of the ordered phase is not excluded in the region far from the boundary [6], although the area of such an ordered region is negligibly small compared with the whole system on the hyperbolic lattice. The situation is similar to that of the statistical models on the Cayley tree, where its deep inside can be regarded as the Bethe lattice [9]. Shima *et al.* studied the Ising model on the hyperbolic lattice by the MC simulations, and observed the mean-field like phase transition deep inside the system [10, 11]. The mean field behavior is in accordance with theoretical studies of phase transition in the infinitely large hyperbolic lattices [12, 13]. It can be

expected that such an order also appears in the case of the XY-model and the clock models.

In this paper we study $N(\geq 3)$ -state clock models on the pentagonal lattice [14] up to $N = 30$ by use of the CTMRG method [15, 16, 17] modified for systems on the hyperbolic lattices [18, 19]. The internal energy and the spontaneous magnetization *at the center of sufficiently large systems* are calculated numerically. In order to judge the presence of an ordered state deep inside the system, we impose the ferromagnetic boundary conditions at the beginning of the iterative calculation of the CTMRG method. As we show in the following, the obtained results support the existence of the mean-field like phase transition for all the N even in the limit $N \rightarrow \infty$, where the system coincides with the classical XY model.

In the next section we introduce geometry of the pentagonal lattice and consider the N -state clock model on it. A brief explanation of the CTMRG method is presented. In Sec. III we show numerical results on the spontaneous magnetization, the internal energy, and the specific heat. We summarize the observed phase transition.

II. CLOCK MODELS ON PENTAGONAL LATTICE

We consider the 2D lattice shown in Fig. 1, which is a tessellation of regular pentagons. The lattice is in a curved plane with a constant negative scalar curvature. Therefore, the Hausdorff dimension of the lattice is infinite. For a technical reason in the CTMRG method, we have chosen the lattice with the coordination number four [14]. Two geodesics drawn by the thick arcs cross one another at a site labeled by θ_1 . By these two arcs the whole lattice is divided into four equivalent parts called the quadrants or the corners.

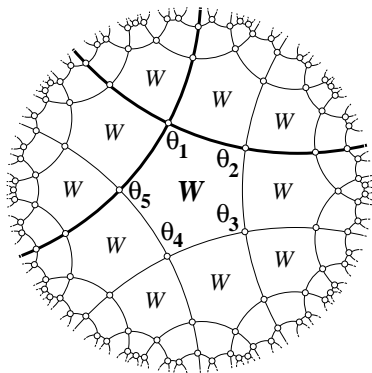


FIG. 1: The pentagonal lattice drawn in the Poincaré disc. The open circles represent the N -state spin variables θ_i . Two geodesics drawn by thick arcs divide the system into four equivalent quadrants.

Let us introduce the N -state clock model on the pentagonal lattice. On each lattice site there is an N -state spin variable θ_i where i is the site index. The possible values of θ_i are $2\pi\xi/N$ with $\xi = 0, 1, 2, \dots, N-1$. We consider the *angle* θ_i as the internal degree of freedom. Therefore, θ_i has nothing to do with the lattice geometry. If there are only ferromagnetic interactions between neighboring spin pairs, the Hamiltonian of the N -state clock model is written as

$$\mathcal{H} = -J \sum_{\langle ij \rangle} \cos(\theta_i - \theta_j), \quad (1)$$

where $J > 0$ is the coupling constant. The summation runs over all the nearest-neighbor pairs $\langle ij \rangle$. The case $N = 2$ is nothing but the Ising model with coupling interaction J and this case has been studied [18, 19]. The case $N = 4$ can be reduced to the Ising model with the coupling $J/2$. We thus chiefly discuss the case $N = 3$, which is equivalent to the 3-state Potts model, and the cases $N \geq 5$ in the following. In order to observe the phase transition deep inside the system, we impose the ferromagnetic boundary conditions so that all the spin variables at the system boundary are aligned in the direction $\theta = 0$.

For convenience we represent this clock model as a special case of the interaction-round-a-face (IRF) model on the hyperbolic lattice. For instance, let us label the spins around a pentagon as shown in Fig. 1. The IRF weight W , which is the local Boltzmann weight corresponding to this pentagon, is obtained as

$$W(\theta_1 \theta_2 \theta_3 \theta_4 \theta_5) = \prod_{i=1}^5 \exp \left\{ \frac{J \cos(\theta_i - \theta_{i+1})}{2 k_B T} \right\}, \quad (2)$$

where $\theta_6 \equiv \theta_1$. Having the IRF weight W thus defined, we can express the partition function of the whole system

$$\mathcal{Z} = \sum_{\{\theta\}} \prod W, \quad (3)$$

where the product is taken for all the IRF weights in the pentagonal lattice. The sum $\sum_{\{\theta\}}$ is taken over all spin configurations.

In order to discuss the phase transition on the hyperbolic lattice, let us consider a system whose size (or diameter) L is far larger than the correlation length ξ . We divide the system into two parts, the boundary area (BA) and the deep inside area (DIA). The former, BA, is a ring-shaped area, where all the sites in the area are within the distance of the order of ξ from the system boundary. The latter, DIA, is the rest of the system, which we analyze in the following. Because of the hyperbolic geometry, the portion of the BA with respect to the whole system is always finite even in the limit $L \rightarrow \infty$. The situation is similar to that of the Cayley tree [9]. Thus the thermodynamic property of the whole system is always affected by the boundary condition, especially in low temperature [7, 8]. When ξ is finite, it is possible to consider the thermodynamics of the DIA, discarding the thermodynamic contribution from the BA, since we have assumed $L \gg \xi$ and therefore the size of the DIA is sufficiently large. When we collect numerical data of the DIA, we always treat sufficiently large systems that satisfy $L \gg \xi$, choosing such temperatures for which ξ is at most of the order of 1000. We then detect the phase transition in the DIA by extrapolation from both low- and high-temperature sides.

We introduce Baxter's corner transfer matrix (CTM) C , which represents the Boltzmann weight of a quadrant of the system [9]. The partition function \mathcal{Z} is then expressed as $\text{Tr } C^4$, i.e., as the trace of the *density matrix* $\rho = C^4$. Applying the concept of the density matrix renormalization [20, 21, 22], a precise approximation of \mathcal{Z} can be obtained for large scale systems by way of iterative numerical calculations [15, 16, 17]. These are the outline of the CTMRG method, which can be applied to statistical models on hyperbolic lattices [18, 19].

After we obtain the density matrix ρ for a sufficiently large system, we can calculate the expectation values at the center of the system, which represent the thermodynamics deep inside the system. For example, we can obtain the spontaneous magnetization

$$\mathcal{M}^{(N)} = \text{Tr} [\cos(\theta_c) \rho] / \text{Tr } \rho, \quad (4)$$

where θ_c represents the spin at the center of the system, and the internal energy per bond

$$\mathcal{E}^{(N)} = -J \text{Tr} [\cos(\theta_c - \theta'_c) \rho] / \text{Tr } \rho, \quad (5)$$

where θ'_c is the neighboring spin next to θ_c . The specific heat $\mathcal{C}^{(N)}$ can be obtained by taking the numerical derivative of $\mathcal{E}^{(N)}$ with respect to temperature T . It should be noted that $\mathcal{M}^{(N)}$, $\mathcal{E}^{(N)}$, and $\mathcal{C}^{(N)}$ are not thermodynamic functions of the whole system but are those of the area deep inside the system.

It has been known that the decay of the density matrix eigenvalues is very fast for models on the hyperbolic lattices [18, 19]. The clock model under study has the

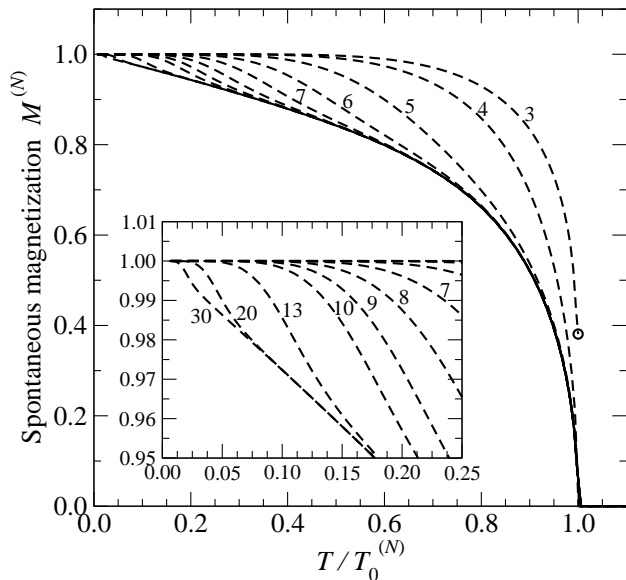


FIG. 2: Temperature dependence of the spontaneous magnetization $\mathcal{M}^{(N)}$ for $3 \leq N \leq 30$. The open circle denotes the discontinuity in $\mathcal{M}^{(3)}$.

same feature in common. Therefore, it is sufficient to keep a very small number of the degree of freedom for the block spin variable m in the formalism of CTMRG. Typically, we keep $m \approx 2N$ states. We checked that further increase of m does not improve numerical precision in $\mathcal{M}^{(N)}$ and $\mathcal{E}^{(N)}$ any more, even at the vicinity of the phase transition.

III. NUMERICAL RESULTS

Throughout this section, we take the coupling constant J in Eq. (1) to the unit of energy. For all the cases $N \geq 2$, we observe phase transition, where the transition temperatures $T_0^{(N)}$ are listed in Table I. Note that $T_0^{(N)}$ converges to $T_0^{(\infty)}$ very fast with respect to N .

Figure 2 shows the spontaneous magnetization $\mathcal{M}^{(N)}$ with respect to the rescaled temperature $T/T_0^{(N)}$. (Under this rescaling, $\mathcal{M}^{(2)}$ and $\mathcal{M}^{(4)}$ are identical.) If $N = 3$, the magnetization is discontinuous at $T_0^{(3)}$. The 3-state clock model, which is equivalent to the 3-state Potts model, exhibits the first order phase transition if the system is on the pentagonal lattice. This is a kind of mean-field behavior, since it is well known that the mean-field approximation applied to the 3-state Potts model on 2D lattices show the first order phase transition [23]. In the vicinity of $T_0^{(N)}$ the magnetization $\mathcal{M}^{(N)}$ rapidly converges to the large N limit $\mathcal{M}^{(\infty)}$. The inset of Fig. 2 displays the low-temperature behavior of $\mathcal{M}^{(N)}$ in details. Note that in the limit $N \rightarrow \infty$ the magnetization $\mathcal{M}^{(N)}$ decreases linearly with T at very low temperatures. Figure 3 shows the square of $\mathcal{M}^{(N)}$ with respect

TABLE I: The transition temperatures $T_0^{(N)}$, the critical exponents β , and positions of the specific heat maximum $T_{\text{Sch}}^{(N)}$.

N -clock	$T_0^{(N)}$	β	$T_{\text{Sch}}^{(N)}$
2	2.7991	0.5	—
3	1.6817	—	—
4	1.3995	0.5	—
5	1.3659	0.5	—
6	1.3625	0.5	0.62948
7	1.3623	0.5	0.46295
8	1.3622	0.5	0.35676
9	1.3622	0.5	0.28357
10	1.3622	0.5	0.22997
13	1.3622	0.5	0.13761
20	1.3622	0.5	0.05864
30	1.3622	0.5	0.02600

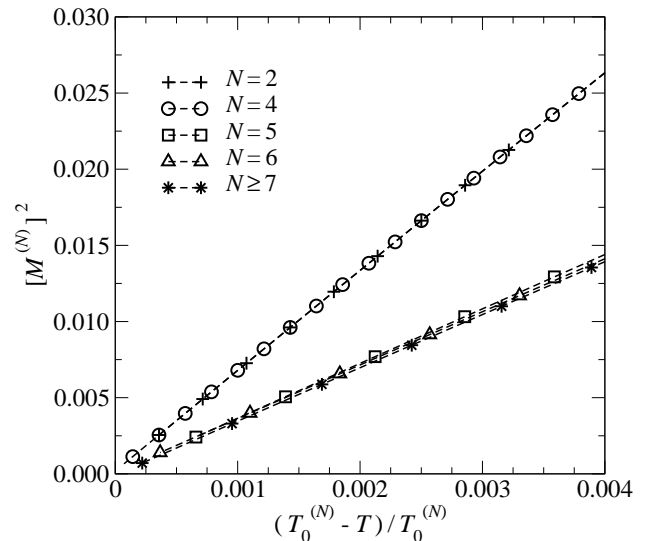


FIG. 3: Square of $\mathcal{M}^{(N)}$ with respect to $(T_0^{(N)} - T)/T_0^{(N)}$.

to $t = (T_0^{(N)} - T)/T_0^{(N)}$ for the cases other than $N = 3$. It is obvious that the scaling relation $\mathcal{M}^{(N)} \propto t^\beta$ is satisfied with the exponent $\beta = \frac{1}{2}$.

Figure 4 shows the internal energy $\mathcal{E}^{(N)}$. There is a finite jump in $\mathcal{E}^{(3)}$ at $T_0^{(3)}$, where the latent heat per bond $\mathcal{L} = \mathcal{E}_+^{(3)} - \mathcal{E}_-^{(3)}$ is 0.078. Analogously to the magnetization $\mathcal{M}^{(N)}$, the $\mathcal{E}^{(N)}$ is linear in T at low-temperature region in the limit $N \rightarrow \infty$.

Figure 5 shows the rescaled specific heat $C^{(N)}/C_{\text{max}}^{(N)}$, where $C_{\text{max}}^{(N)}$ is the specific heat at $T_0^{(N)}$, with respect to the rescaled temperature $T/T_0^{(N)}$. Evidently, a discontinuity in the specific heat is observed for the cases $N = 2$ and $N \geq 4$. Thus, the second order phase transition has the mean-field nature. There is no indication of the BKT transition that is observed for clock models on flat

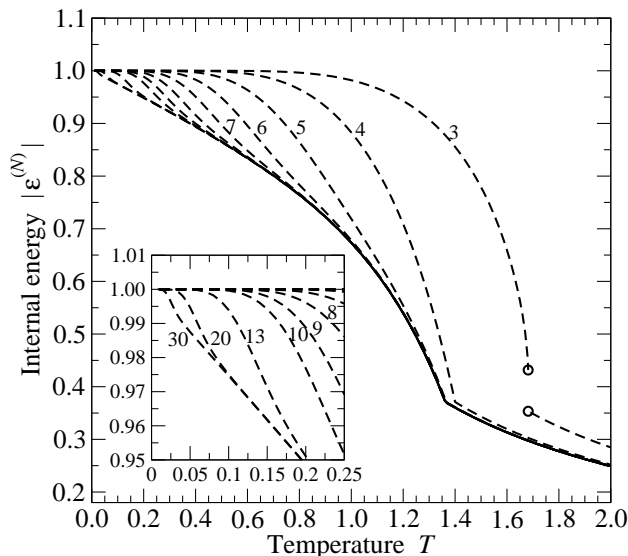


FIG. 4: The absolute value of the internal energy $|\mathcal{E}^{(N)}|$. The open circles denote the jump in the case $N = 3$.

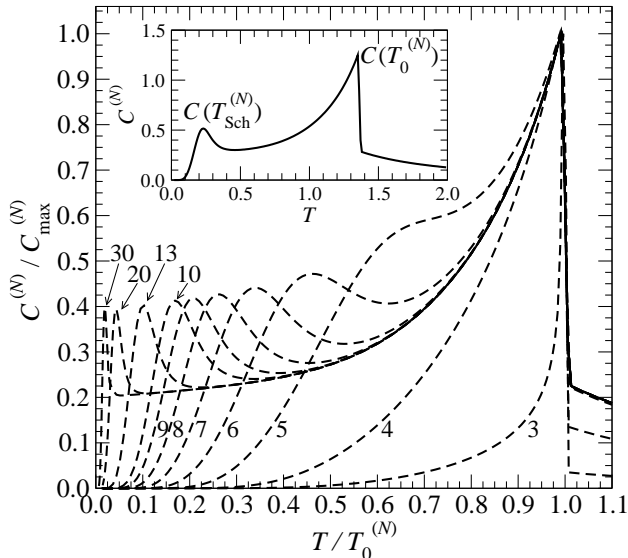


FIG. 5: The rescaled specific heat $C^{(N)}/C_{\max}^{(N)}$ versus the rescaled temperature $T/T_0^{(N)}$. The inset shows a typical example for the case $N = 10$ without rescaling.

2D lattices [24].

When N is larger than 5, we observe the Schottky type peak in the specific heat. Figure 6 shows the N dependence of the Schottky peak position $T_{\text{Sch}}^{(N)}$. As it is shown, $T_{\text{Sch}}^{(N)}$ is proportional to $1/N^2$. This is qualitatively in accordance with the energy scale of local excitation $2(2\pi/N)^2 J$ from the completely ordered state. It is thus concluded that the Schottky peak disappears in the limit $N \rightarrow \infty$ and that the specific heat of the classical XY model on the pentagonal lattice remains finite even at $T = 0$.

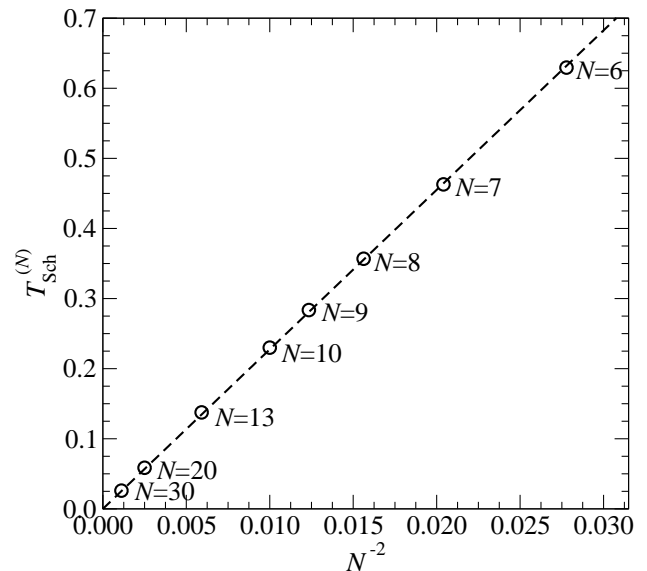


FIG. 6: The Schottky peak position $T_{\text{Sch}}^{(N)}$ versus $1/N^2$.

IV. CONCLUSIONS

We have studied the N -state clock models on the pentagonal lattice, which is a typical example of the hyperbolic lattices. The phase transition deep inside the system is observed by use of the CTMRG method. From the critical exponent $\beta = \frac{1}{2}$ for the spontaneous magnetization and the jump in the specific heat, we conclude that the phase transition for $N = 2$ and $N \geq 4$ is mean-field like, provided that the ferromagnetic boundary conditions are imposed. The Hausdorff dimension, which is infinite for the hyperbolic lattices, is essential in the observed critical behavior. We conjecture that the phase transition deep inside the system is also present for systems with free boundary conditions.

In the case when $N = 3$, where the system is equivalent to the 3-state Potts model, we observed the first-order phase transition. Since the q -state Potts model tends to exhibit the first-order transition for larger q [23], it is expected that the transition of $q \geq 3$ Potts models on the pentagonal lattice is of the first order. We have partially confirmed the behavior for several values of q and we conjecture that the transition is of the first order on any kind of hyperbolic lattices when $q \geq 3$.

We observed stable ferromagnetic states below $T_0^{(N)}$ even in the continuous limit $N \rightarrow \infty$. This fact does not contradict to the Mermin-Wagner theorem [1] since the pentagonal lattice is not on the flat 2D plane. The vortex energy on hyperbolic lattices might be larger than that on the flat lattice. The difference may elucidate the absence of the BKT phase transition on the pentagonal lattice.

Acknowledgments

The Slovak Agency for Science and Research grant APVV-51-003505 and Slovak VEGA grant No.

2/6101/27 are acknowledged (A.G. and R.K.). This work is also partially supported by Grant-in-Aid for Scientific Research from Japanese Ministry of Education, Culture, Sports, Science and Technology (T.N. and A.G.).

-
- [1] N. D. Mermin and H. Wagner, *Phys. Rev. Lett.* **17**, 1133 (1966).
- [2] Z. L. Berezinskii, *Zh. Eksp. Teor. Fiz.* **61**, 11446 (1971).
- [3] J. M. Kosterlitz and D. J. Thouless, *J. Phys. C* **6**, 1181(1973); J. M. Kosterlitz, *J. Phys. C* **7**, 1046 (1974).
- [4] S. K. Baek, P. Minnhagen, and B. J. Kim, *Euro Phys. Lett.* **79**, 26002 (2007).
- [5] F. Sausset and G. Tarjus *J. Phys. A: Math. Gen.* **40** 12873 (2007).
- [6] J.C. Anglès d'Auriac, R. Mélin, P. Chandra and B. Douçot *J. Phys. A: Math. Gen.* **34** 675 (2001).
- [7] N. Anders and C. Chris Wu, *Combinatorics, Probability and Computing* **14**, 523 (2005).
- [8] C. Chris Wu, *J. Stat. Phys.* **100**, 893 (2000).
- [9] R. J. Baxter, *Exactly solved models in statistical mechanics* Academic Press, London (1982).
- [10] H. Shima and Y. Sakaniwa, *J. Phys. A* **39**, 4921(2006).
- [11] I. Hasegawa, Y. Sakaniwa, and H. Shima, *preprint in cond-mat/0612509*.
- [12] R. Rietman, B. Nienhuis, and J. Oitmaa, *J. Phys. A* **25**, 6577 (1992).
- [13] B. Doyon and P. Fonseca *J. Stat. Mech.* P07002 (2004).
- [14] The CTMRG method requires the presence of geodesics in the geometrical structure of the lattice. Thus the coordination number q should be even. Both the pentagonal lattice under study and the heptagonal lattice studied by Baek *et al.* are on the hyperbolic plane, and the XY model on these lattice may belong to the same universality class.
- [15] T. Nishino and K. Okunishi, *J. Phys. Soc. Jpn.* **65**, 891 (1996).
- [16] T. Nishino, K. Okunishi, and M. Kikuchi, *Phys. Lett. A* **213**, 69 (1996).
- [17] T. Nishino and K. Okunishi, *J. Phys. Soc. Jpn.* **66**, 3040 (1997).
- [18] K. Ueda, R. Krčmar, A. Gendiar, and T. Nishino, *J. Phys. Soc. Jpn.* **76**, 084004 (2007).
- [19] R. Krčmar, A. Gendiar, K. Ueda, and T. Nishino, *J. Phys. A: Math. Theor.* **41** 125001 (2008).
- [20] S. R. White, *Phys. Rev. Lett.* **69**, 2863 (1992).
- [21] S. R. White, *Phys. Rev. B* **48**, 10345 (1993).
- [22] U. Schollwöck, *Rev. Mod. Phys.* **77**, 259 (2005).
- [23] F. Y. Wu, *Rev. Mod. Phys.* **54**, 235 (1982).
- [24] M.S.S. Challa and D.P. Landau, *Phys. Rev. B* **33**, 437 (1986).